Available online at www.sciencedirect.com
SCIENCE DIRECT®
Journal of Nuclear Materials 355 (2006) 131–135
journal of nuclear materials
www.elsevier.com/locate/jnucmat

Xenon versus helium behavior in UO_2 single crystals: A TEM investigation

G. Sattonnay [a,b,*], L. Vincent [a], F. Garrido [a], L. Thomé [a]

[a] Centre de Spectrométrie Nucléaire et de Spectrométrie de Masse, CNRS-IN2P3, Université Paris-Sud, Bât. 108, F-91405 Orsay Campus, France
[b] Laboratoire d'Etude des Matériaux Hors Equilibre, ICMMO, CNRS UMR 8647, Université Paris-Sud, Bât. 410, F-91405 Orsay Campus, France

Received 5 October 2005; accepted 18 April 2006

Abstract

The behavior of He and Xe implanted into UO_2 single crystals is studied by *in situ* TEM experiments before and after annealing up to 700 °C. TEM micrographs show that annealing induces the formation of noble-gas bubbles in both cases. However, the size (~25 nm for He and 3–5 nm for Xe) and the nucleation temperature (~600 °C for He and ~400 °C for Xe) of bubbles depend on implanted species. These results are explained by the radiation damage produced by ion implantation (different by a factor of 100 for the two elements) and the diffusion mechanisms involved in each case.

1. Introduction

The knowledge of the physico-chemical properties of uranium dioxide (UO_2) is of prime importance since this material is the today's fuel for nuclear energy production. After irradiation in the reactor, the spent fuel contains large concentrations (a few atomic percent) of volatile fission products (Xe, Kr, I, etc.) and α-particle emitters (^{238}Pu, ^{242}Cm, ^{244}Cm, ^{241}Am, etc). Due to their low solubility in the UO_2 lattice, fission products and helium atoms produced by the α-decay of actinides tend to precipitate, either during the fuel irradiation for the former species or in fuel storage conditions, at lower temperature, for the latter ones [1]. This precipitation induces a swelling phenomenon which affects the mechanical properties of the fuel. The swelling may cause the fracture of the material and thus may produce a dramatic release of radiotoxic elements into the environment. Therefore, the study of the behavior of volatile fission products and helium in UO_2 reveals a high technological interest.

The problem of fission gas release (mostly Xe and Kr) from UO_2 pellets has been extensively investigated since the late 1960s (see for example Refs. [2–7]). Conversely only a few studies have been performed in order to understand the behavior of He

* Corresponding author. Address: Centre de Spectrométrie Nucléaire et de Spectrométrie de Masse, CNRS-IN2P3, Université Paris-Sud, Bât. 108, F-91405 Orsay Campus, France. Tel.: +33 1 69 157037; fax: +33 1 69 154819.
E-mail address: gael.sattonnay@lemhe.u-psud.fr (G. Sattonnay).

0022-3115/$ - see front matter © 2006 Elsevier B.V. All rights reserved.
doi:10.1016/j.jnucmat.2006.04.013

Table 1
Implantation parameters for He and Xe ion implantations

Ion	Energy (keV)	Fluence (cm^{-2})	R_p (nm)	ΔR_p (nm)	c (at.%)	E_v (eV nm^{-1})	dpa
He	7	7×10^{15}	40	21	1.3	30	0.6
Xe	260	8×10^{15}	47	22	1.5	4×10^{3}	63

The atomic concentration (c), the energy deposited in nuclear collisions (E_v) and the number of dpa are calculated at R_p.

atoms in UO_2 sintered disks [8–10]. The main purpose of the present work was to compare the formation of helium and xenon precipitates in UO_2 single crystals submitted to high-temperature annealing and to interpret the experimental results by reference to the solubilities, irradiation damage and diffusion mechanisms of each atom. The use of single crystals is justified by the necessity to investigate the intrinsic behavior of He or Xe without the effects of grain boundaries. Helium and xenon atoms were incorporated into the UO_2 crystals by ion implantation, a technique which provides a good monitoring of the depth distribution and concentration of implanted species. Transmission electron microscopy (TEM) experiments were used to observe the formation of both radiation damage and noble-gas precipitates during *in situ* annealing steps.

2. Experimental procedures

Small pieces cut from a UO_2 single crystal ({1 1 0} orientation) were annealed in a H_2/Ar (10%) gas mixture at 1400 °C in order to obtain the proper oxygen-to-metal ratio (O/U ~2.0), and were then mechanically thinned with the Tripod technique to form a wedge of 1-5 μm thickness. Electron transparent thin foils were obtained by a final polishing with the Manley technique [11], which offers an interesting alternative to ion milling [12] for the reduction of radiation damage.

UO_2 thin foils were implanted with either 7 keV He^+ ions (fluence: 7×10^{15} cm^{-2}) or 260 keV Xe^{2+} ions (fluence: 8×10^{15} cm^{-2}) delivered by the IRMA facility of the CSNSM in Orsay. The ion energies and fluences were chosen in order to obtain a concentration of implanted species of the order of 1 at.% in the middle of the foils; the dose-rate was always kept below 1 μA cm^{-2} in order to minimize target heating during implantation. The SRIM code [13] was used in order to evaluate the ion projected ranges (R_p) and range stragglings (ΔR_p), as well as the energies deposited in nuclear collisions (E_v) and the numbers of displacements per atom (dpa) created at R_p at the final fluences Table 1. These calculations were performed with a theoretical target density of 10.95 g cm^{-3} and displacement threshold energies of 40 eV for U atoms and 20 eV for O atoms.

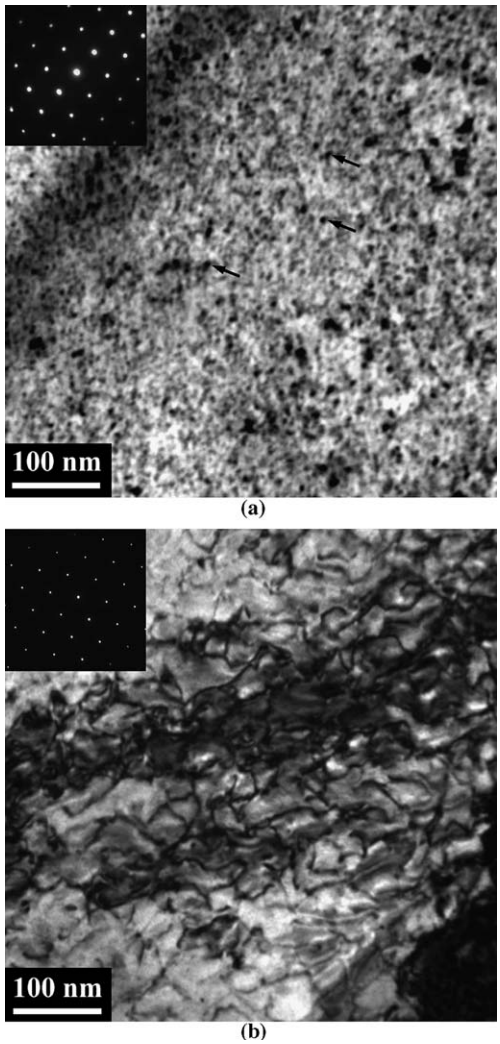

Fig. 1. TEM images of ion-implanted UO_2 single crystals. Insets show diffraction patterns recorded with the electron beam parallel to the [$\bar{1}$ 1 0] axis. (a) 7 keV He ions (fluence: 7×10^{15} cm^{-2}). Dislocation loops (black dots) are indicated by arrows. (b) 260 keV Xe ions (fluence: 8×10^{15} cm^{-2}).

Isochronal anneals were carried out *in situ* in a 120 keV Philips CM12 TEM, equipped with a Gatan™ camera and a Digital Micrograph™ image recording system, from 100 up to 700 °C (uncertainties of ±20 °C) with temperature steps of 100 °C and annealing times of 15 min.

3. Results

TEM images recorded on ion-implanted UO_2 crystals (before annealing) are displayed in Fig. 1. A high density of black dots (with a mean size of 5 nm) is exhibited on the sample implanted with He ions (Fig. 1(a): arrows). Similar dots were previously observed on UO_2 irradiated with neutrons and electrons [14,15] and were identified as dislocation loops. In addition to dislocation loops, the sample implanted with Xe ions exhibits a network of tangled dislocations (Fig. 1(b)), which are expected to be the result of the coalescence of dislocation loops [16,17]. The diffraction patterns (shown in the insets of Fig. 1) indicate that both samples remain crystalline after ion implantation.

Figs. 2 and 3 present TEM images recorded on UO_2 crystals submitted, respectively, to He and Xe ion implantation and annealing. In both cases annealing has induced the formation of noble-gas bubbles. However, the size of bubbles and the temperature at which bubbles nucleate strongly depend on implanted species: ~25 nm and 600 °C for He; 3–5 nm and 400 °C for Xe. The TEM image of Fig. 2(a) shows that a white-line contrast is observed for some He bubbles (see arrows). This white-line contrast is a type of displacement fringe which indicates that the interface of bubbles is curved. The TEM image of Fig. 2(b) recorded in an approximate two-beam condition show that each He bubble presents a line of no-contrast normal to the diffraction vector. This feature is typical of isotropic

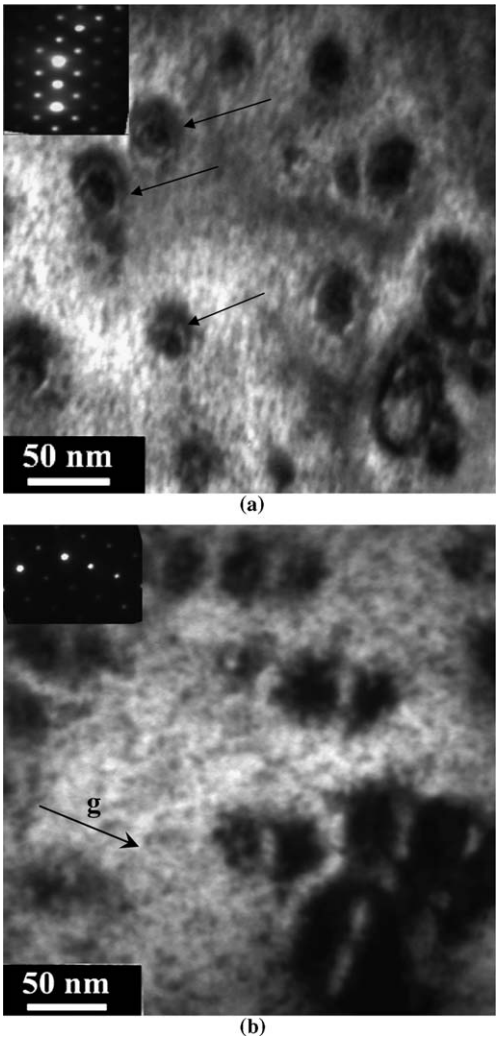

Fig. 2. TEM image and diffraction pattern of UO_2 single crystals implanted with He ions (fluence: 7×10^{15} cm^{-2}) and annealed at 600 °C, (a) registered with the electron beam almost parallel to the $[\bar{1}10]$ axis. (b) Recorded in two-beam condition with $g = [111]$. He bubbles are indicated by arrows.

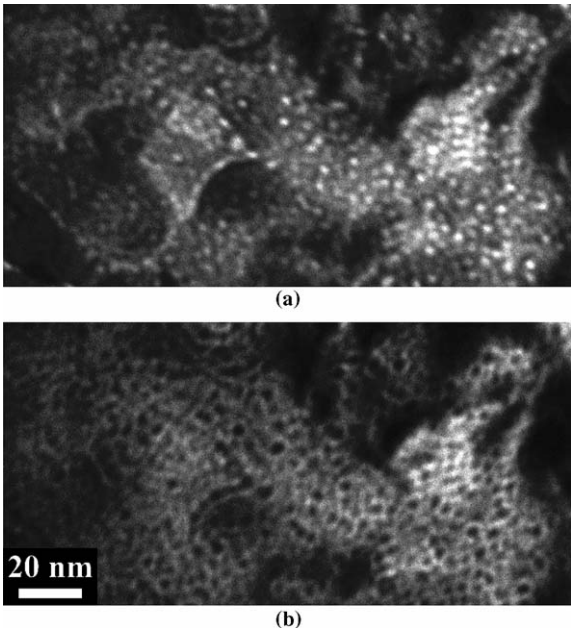

Fig. 3. TEM images of UO_2 single crystals implanted with Xe ions (fluence: 8×10^{15} cm^{-2}) and annealed at 400 °C, registered by overfocusing (a) and underfocusing (b) the objective lens.

strain-field contrasts (at least for this orientation) [18]. On the other hand Xe bubbles were characterized by contrast changes on underfocusing and overfocusing the objective lens (Fig. 3) and no strain-field contrast is observed.

It is worth noting that below the indicated annealing temperatures (600 °C for He and 400 °C for Xe), no noble-gas bubbles are visible on the TEM images. Moreover, no increase of the size of bubbles with increasing annealing temperature (up to 750 °C) or time (up to several hours) is observed.

4. Discussion

The TEM results show that the precipitation of He or Xe atoms in UO_2 occurs above a threshold temperature, T_c, which strongly depends on implantation conditions ($T_c = 600$ °C for 7 keV He and 400 °C for 260 keV Xe). A second huge difference is the size of the noble-gas bubbles formed which are much smaller for Xe implantation (3–5 nm) than for He (~25 nm). Moreover, in a recent paper, Sattonnay et al. [19] showed that the size of He bubbles can be even much larger (~200 nm) when the ion fluence is increased up to 2.6×10^{16} cm^{-2}, leading to a He concentration of ~5 at.% (instead of ~1 at.% in the present work).

These experimental results will be discussed below by taking into account three parameters: the He and Xe solubilities in UO_2, the irradiation damage and the diffusion mechanisms.

The solubilities of the two species in the UO_2 matrix are different: Xe is insoluble in UO_2, whereas He is soluble in small quantities [20]. Moreover, He becomes increasingly soluble when the temperature is increased. Thus, the percentage of He atoms available to form bubbles decreases when the temperature increases. In our experiments, the fact that He bubbles are formed at 600 °C at the lowest fluence used (7×10^{15} cm^{-2}) indicates that the He concentration at this fluence (~1 at.%) is above the solubility limit. Nevertheless, all implanted He atoms are not necessarily trapped in bubbles, some of them being dissolved in the matrix (contrarily to Xe atoms). The fact that T_c(He) is higher than T_c(Xe) indicates that Xe apparently diffuses faster than He in ion-implanted UO_2 crystals. This result is at odds with previous data which show that He diffuses faster than Xe in UO_2 fuel pellets [10,21,22]. This discrepancy as well as the difference in the size of noble-gas bubbles formed may be accounted for by the radiation damage induced by ion implantation and the lattice sites occupied by implanted atoms, which both strongly influence the diffusion mechanisms.

Fig. 1 shows that quite different microstructures are formed in UO_2 crystals implanted with noble-gas species, depending on the implantation conditions: isolated dislocation loops in the case of 7 keV He (Fig. 1(a)), a network of tangled dislocations in the case of 260 MeV Xe (Fig. 1(b)). Although He and Xe ion fluences are very close, leading to almost identical noble-gas concentrations in the implanted layer in both cases, this result can be accounted for by the huge difference in the energy deposited in nuclear collisions, leading to very different number of dpa created by incoming ions (Table 1). In a recent paper Thomé et al. measured, by Rutherford backscattering and channeling (RBS/C) experiments, the damage accumulated in cubic yttria-stabilized zirconia single crystals (structure isomorphic of the UO_2 one) irradiated with various noble-gas ions [23]. The results show the presence of several disordering stages scaled with the number of dpa. Actually Xe ion irradiation with fluences higher than $\sim 2 \times 10^{15}$ cm^{-2} (~5 dpa) led to highly disordered crystals (referred to as stage 3), whereas He ion irradiation with fluences lower than 3×10^{16} cm^{-2} led to a very low disorder level (referred to as stage 1), He fluences as high as 8×10^{16} cm^{-2} being required to reach a disorder level characteristic of stage 3. Preliminary RBS/C data recorded on ion-irradiated UO_2 single crystals led to very similar results concerning the disorder production [24]. Thus, the much larger amount of defects created by Xe implantation as compared to He, indicated by SRIM calculations, RBS/C and TEM data, supports Xe mobility at a lower temperature than He.

It has also been shown by lattice location experiments that He atoms occupy octahedral interstitial positions in the UO_2 lattice [25], whereas Xe atoms substitute U atoms [26]. Thus He diffuses probably via an interstitial mechanism as it was observed in yttria-stabilized zirconia [27]. Conversely the diffusion process of substitutional Xe involves certainly the vacancies created by energetic ions as it was shown by Evans in UO_2 implanted with Kr and Xe ions [7]. Actually, several studies suggest that xenon atoms are most likely trapped in neutral trivacancies, a shottky trio consisting of one uranium vacancy and two oxygen vacancies. Ball and Grimes proposed that the xenon diffusion occurs by the association of a second uranium vacancy with the trivacancy trap to form a larger tetravacancy cluster [28]. Thus, the huge amount of radiation-induced

vacancies produced in the case of Xe ion implantation would lead to an enhancement of the Xe diffusion during annealing comparatively to He.

5. Conclusion

A study of the behavior upon annealing of He and Xe implanted into UO_2 single crystals at a concentration of $\sim$ 1 at.% was performed by *in situ* TEM experiments. Noble-gas bubbles with a size $\sim$25 nm for He and 3–5 nm for Xe are formed at annealing temperatures of 600 °C for He and 400 °C for Xe. The decrease of the temperature at which Xe bubbles nucleate comparatively to He ones and the strong difference in the bubble size are likely due to both the radiation damage production, which is different by a factor of 100 between the two species, and the diffusion mechanisms involved in each case. Further experiments have to be performed in order to determine the respective roles of these two factors. For instance, it would be particularly interesting to pre-damage a UO_2 thin film with energetic particles before implanting various fluences of He ions. The defects created by the pre-irradiation could help He atoms to diffuse in order to create bubbles at a lower temperature than that found in the present work. The reverse is certainly also true for Xe. The introduction of impurities via a route which does not lead to the creation of damage (for instance by gas infusion at high pressure) would certainly shift the temperature above which bubbles form towards a higher value. Thus, a modulation of the nucleation temperature of noble-gas bubbles in nuclear matrices could be obtained by varying the amount of radiation defects introduced in the lattice of the investigated material.

Acknowledgement

The authors are grateful to O. Kaitasov for her assistance during ion implantation. This work was partially supported by the GDR NOMADE.

References

[1] W.J. Weber, R.C. Ewing, C.R.A. Catlow, T. Diaz de la Robia, L.W. Hobbs, C. Kinoshita, Hj. Matzke, A.T. Motta, M. Nastasi, E.K.H. Salje, E.R. Vance, S.J. Zinkle, J. Mater. Res. 13 (1998) 1434.
[2] W.F. Mickeley, F.W. Felix, J. Nucl. Mater. 42 (1972) 297.
[3] G.T. Lawrence, J. Nucl. Mater. 71 (1978) 195.
[4] P. Lösönen, J. Nucl. Mater. 280 (2000) 56.
[5] J.A. Turnbull, C.A. Friskney, J. Nucl. Mater. 71 (1978) 238.
[6] V.F. Chkuaseli, Hj. Matzke, J. Nucl. Mater. 223 (1995) 61.
[7] J.H. Evans, J. Nucl. Mater. 188 (1992) 222.
[8] S. Guilbert, T. Sauvage, H. Erramli, M.-F. Barthe, P. Desgardin, G. Blondiaux, C. Corbel, J.P. Piron, J. Nucl. Mater. 321 (2003) 121.
[9] S. Guilbert, T. Sauvage, P. Garcia, G. Carlot, M.-F. Barthe, P. Desgardin, G. Blondiaux, C. Corbel, J.P. Piron, J.-M. Gras, J. Nucl. Mater. 327 (2004) 88.
[10] C. Ronchi, J.P. Hiernaut, J. Nucl. Mater. 325 (2004) 1.
[11] A.J. Manley, J. Nucl. Mater. 15 (1965) 143.
[12] Hj. Matzke, P.G. Lucuta, T. Wiss, Nucl. Instrum. and Meth. B 166&167 (2000) 926.
[13] J.F. Ziegler, J.P. Biersack, U. Littmark, The Stopping and Range of Ions in Solids, Pergamon, New York, 1985.
[14] A.D. Whapham, B.E. Sheldon, Philos. Mag. 12 (1965) 1179.
[15] J. Soulard, J. Nucl. Mater. 135 (1995) 190.
[16] K. Nogita, K. Hyashi, K. Une, K. Fukuda, J. Nucl. Mater. 273 (1999) 302.
[17] T. Sonoda, M. Kinoshita, I.L.F. Ray, T. Wiss, H. Thiele, D. Pellottiero, V.V. Rondinella, Hj. Matzke, Nucl. Instrum. and Meth. B 191 (2002) 622.
[18] M.F. Ashby, L.M. Brown, Philos. Mag. 8 (1963) 1083.
[19] G. Sattonnay, F. Garrido, L. Thomé, Philos. Mag. Lett. 84 (2004) 109.
[20] T. Petit, M. Freyss, P. Garcia, P. Martin, M. Ripert, J.-P. Crocombette, F. Jollet, J. Nucl. Mater. 320 (2003) 133.
[21] Hj. Matzke, Radiat. Eff. 53 (1980) 219.
[22] C. Ronchi, J. Sakellaridis, C. Syros, Sci. Eng. 95 (1987) 282.
[23] L. Thomé, J. Fradin, J. Jagielski, A. Gentils, S.E. Enescu, F. Garrido, Eur. Phys. J. Appl. Phys. 24 (2003) 37.
[24] F. Garrido, L. Thomé, G. Sattonnay, L. Vincent, Nucl. Instrum. and Meth., submitted for publication.
[25] F. Garrido, L. Nowicki, G. Sattonnay, T. Sauvage, L. Thomé, Nucl. Instrum. and Meth. B 219&220 (2004) 196.
[26] Hj. Matzke, A. Turos, J. Nucl. Mater. 188 (1992) 285.
[27] P.M.G. Damen, Hj. Matzke, C. Ronchi, J.-P. Hiernaut, T. Wiss, R. Fromknecht, A. van Veen, F. Labohm, Nucl. Instrum. and Meth. B 191 (2002) 571.
[28] R.G.J. Ball, R.W. Grimes, J. Chemical Society, Faraday Trans. 86 (1990) 1257.